

Critical scalings in thermal colloidal systems near the jamming transition

Lijin Wang and Ning Xu*

CAS Key Laboratory of Soft Matter Chemistry,
Hefei National Laboratory for Physical Sciences at the Microscale & Department of Physics,
University of Science and Technology of China,
Hefei 230026, People's Republic of China.

* e-mail: ningxu@ustc.edu.cn.

arXiv:1112.2429v1 [cond-mat.soft] 12 Dec 2011

Colloids and granular materials jam into amorphous solids at sufficiently large volume fractions [1–5]. A recent study unveils that the first peak of the pair distribution function shows a maximum, g_1^{\max} during the jamming of thermal colloids, but it does not coincide with the dynamically-defined glass transition [1]. Here we claim that the emergence of g_1^{\max} contains important physics by showing that multiple quantities undergo significant changes at the maximum. Surprisingly, these quantities exhibit critical scaling collapse at low temperatures when they are simply scaled by scaling laws at g_1^{\max} , implying the criticality of the $T = 0$ jamming transition. Moreover, in thermal colloidal systems, we find the strong coupling between the isostaticity and plateau in the density of vibrational states, a unique feature at the $T = 0$ jamming transition [6], in the regime where the $T = 0$ jamming transition has not been completely forgotten.

As described by the seminal jamming phase diagram [3], a packing of frictionless spheres interacting via repulsion undergoes the jamming transition at a critical-like volume fraction ϕ_c , denoted as Point J. At $T = 0$, marginally jammed solids near Point J show multiple critical scalings and length scales [6–14]. Although it is still under debate whether ϕ_c has a well-defined value [15–17], all the critical scalings only rely on the distance from Point J, $\phi - \phi_c$ [16]. Interestingly, it has been shown that Point J has great significance in our understanding of the long-standing glass transition problems [14, 18].

The nature of the glass transition remains elusive [19, 20]. One of the main difficulties is the lack of proper order parameters to exhibit diverging static correlation length. Although some quantities have been proposed recently, none of them can be generally applied to different systems [21, 22]. This difficulty originates from the structural similarity between glass-forming liquids and glasses, which obscures observable structural changes during the glass transition.

Recently, a structural change has been observed in experiments and simulations of thermal colloidal systems undergoing the glass transition [1], reminiscing the structural signature of the $T = 0$ jamming transition [23, 24]. At Point J, particles are just in contact, which induces a δ -function of the first peak of the pair distribution function, $g(r)$. Upon compression away from Point J, the

height of the first peak of $g(r)$, g_1 is inversely scaled with $\phi - \phi_c$, because g_1 is inversely proportional to the particle overlap which grows linearly with $\phi - \phi_c$ [23]. At $T > 0$, g_1 reaches a maximum value, g_1^{\max} at a temperature dependent volume fraction (pressure), ϕ_j (p_j). For the model systems used here and in Ref. [1] (see Methods), simple analysis suggests that ϕ_j and g_1^{\max} approaches ϕ_c and infinity in the $T = 0$ limit according to the scaling laws: $\phi_j - \phi_c \sim T^{1/\alpha}$ and $g_1^{\max} \sim (\phi_j - \phi_c)^{-1} \sim T^{-1/\alpha}$, where α determines the inter-particle potential. Correspondingly, $T_j \sim p^{\alpha/(\alpha-1)}$ at ϕ_j , which, however, does not agree with the pressure dependence of the glass transition temperature defined by the divergence of the relaxation time: $T_g \sim p$ [25].

It remains an open question whether the emergence of g_1^{\max} is merely the thermal vestige of the $T = 0$ jamming transition. If not, does it imply any physical significance in the formation of amorphous solids? What features of the $T = 0$ jamming transition would persist at $T > 0$ and in what manner?

Figure 1 indicates that the emergence of g_1^{\max} is accompanied with apparent material property changes. In a wide range of temperatures, both $\phi - \phi_c$ and potential energy per particle, V show distinct pressure dependence on two sides of the crossover pressure p_j . At $p > p_j$,

$$\phi - \phi_c \sim \left(\frac{p}{\phi^2}\right)^{1/(\alpha-1)}, \quad (1)$$

$$V - \frac{zT}{4} \sim (\phi - \phi_c)^\alpha \sim \left(\frac{p}{\phi^2}\right)^{\alpha/(\alpha-1)}, \quad (2)$$

where $\phi_c = 0.649 \pm 0.002$ for both harmonic ($\alpha = 2$) and Hertzian ($\alpha = 2.5$, shown in Supplementary Information) repulsions, and z is the average coordination number which will be discussed in detail later. Here we subtract V by the thermal contribution, $\frac{1}{2}k_B T \frac{z}{2}$, assuming equipartition [1], where the Boltzmann constant k_B is set to be one, in order to make direct comparison to the scaling of V at $T = 0$. We correct the widely accepted scaling $p \sim (\phi - \phi_c)^{\alpha-1}$ [8] to Equation 1 simply derived from $V \sim (\phi - \phi_c)^\alpha$ and $p = \phi^2 \frac{dV}{d\phi}$, because away from ϕ_c the variation of ϕ must be considered to explain the data correctly. At $p > p_j$, the critical scalings at $T = 0$ are recovered. At $p < p_j$, however, the jamming-like scalings break down, indicating the notable change of the material properties across p_j . Furthermore, our data show

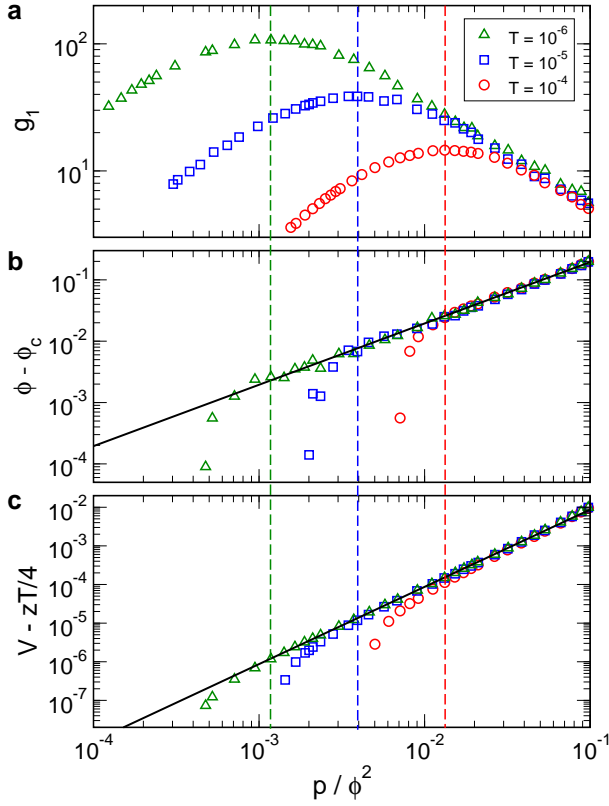


Figure 1 | Temperature and pressure dependence of the volume fraction and potential energy near the emergence of g_1^{\max} . **a**, The height of the first peak of the pair distribution function, g_1 , **b**, volume fraction difference from the $T = 0$ jamming transition, $\phi - \phi_c$, and **c**, potential energy per particle subtracting the thermal contribution, $V - zT/4$ versus the pressure divided by the square of the volume fraction, p/ϕ^2 for systems with harmonic ($\alpha = 2$) repulsion. The black lines in **b** and **c** show the scalings in marginally jammed solids at $T = 0$: $\phi - \phi_c \sim p/\phi^2$, and $V \sim (p/\phi^2)^2$. The dashed lines mark the location of g_1^{\max} .

that

$$g_1^{\max} \sim (\phi - \phi_c)^{-\gamma} \sim \left(\frac{p}{\phi^2}\right)^{-\gamma/(\alpha-1)}, \quad (3)$$

(see Figure 6 of Supplementary Information), where $\gamma = 0.90 \pm 0.02$ which deviates from 1 as discussed above probably due to nonlinear or thermal effects.

A close look at the potential energy (see Figure 7 of Supplementary Information) unveils another interesting phenomenon: $V \approx \frac{3}{2}k_B T$ at p_j . This is consistent with our observation (see Figure 5 and Figure 9 of Supplementary Information) that

$$T_j \sim \left(\frac{p}{\phi^2}\right)^{\alpha/(\alpha-1)}. \quad (4)$$

At $p > p_j$, the potential energy dominates the kinetic energy, so that the thermal motion is hard to cause significant configuration change of jammed states and the

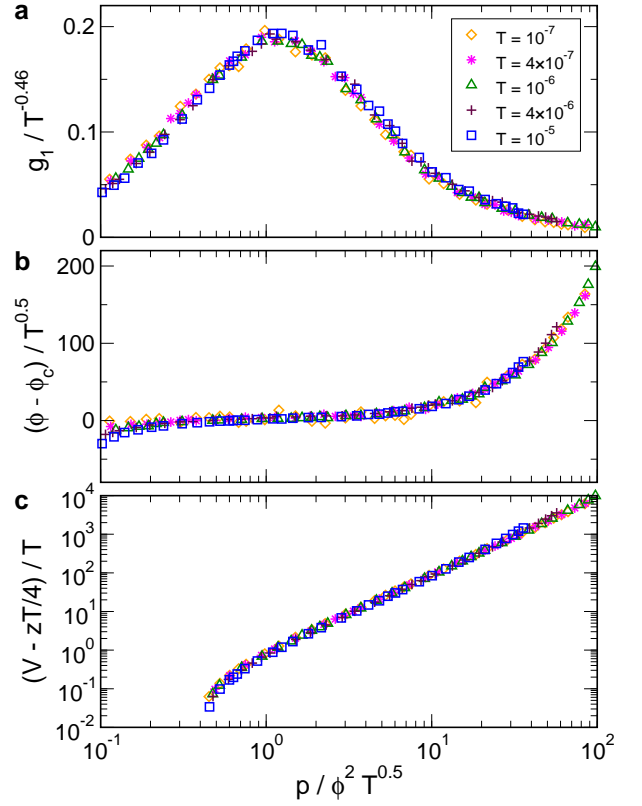


Figure 2 | Critical scaling collapse of the quantities shown in **Figure 1** at low temperatures. **a**, The height of the first peak of the pair distribution function, g_1 scaled by $T^{-0.46}$, **b**, volume fraction difference from the $T = 0$ jamming transition, $\phi - \phi_c$ scaled by $T^{0.5}$, and **c**, potential energy per particle subtracting the thermal contribution, $V - zT/4$ scaled by T versus the scaled pressure $p/\phi^2 T^{0.5}$ for systems with harmonic ($\alpha = 2$) repulsion.

jamming-like scalings thus hold. At $p < p_j$, the kinetic energy wins. The thermal motion has noticeable effects on the system performance. Therefore, the emergence of g_1^{\max} and the corresponding material property changes do not happen by chance, but have explicit physical origins.

Equations (1)–(3) imply the criticality of Point J viewed in thermal colloidal systems. To our surprise, by scaling all the quantities in **Figure 1** using Equations (1)–(4), we obtain nice scaling collapse of the original low-temperature data on both sides of p_j onto a general functional form, as shown in **Figure 2**:

$$\xi = T^{\nu_\xi} f_\xi \left(\frac{p}{\phi^2 T^{(\alpha-1)/\alpha}} \right), \quad (5)$$

where ξ denotes g_1 , $\phi - \phi_c$, and $V - \frac{zT}{4}$, with $\nu_\xi = -\gamma/\alpha$, $1/\alpha$, and 1, respectively. Equation (5) implies the criticality at $T = 0$ and $p = 0$. Note that the scaling collapse is simply derived from the scaling laws at p_j , while such a crossover approaches Point J in the $T = 0$ and $p = 0$ limit. Our finding here strongly supports the criticality of Point J, in agreement with other approaches [12, 13]. The scaling collapse conveys important information of

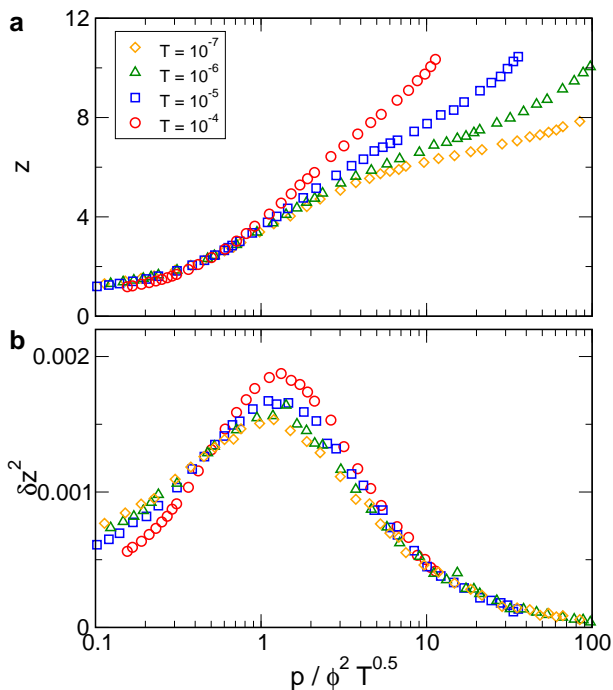


Figure 3 | Temperature and pressure dependence of the coordination number and its fluctuation. **a**, Coordination number, z , and **b**, mean square fluctuation of the coordination number, δz^2 versus the scaled pressure $p/\phi^2 T^{0.5}$ for systems with harmonic ($\alpha = 2$) repulsion.

the low-temperature properties of the glass-formers in the vicinity of Point J, not just trivially reflecting the behaviors at $T = 0$.

One of the special features of the $T = 0$ jamming transition at Point J is the isostaticity, i.e. the average coordination number z is equal to the isostatic value $z_c = 2d$, where d is the dimension of space. In marginally jammed solids, the coordination number increases with the compression according to $z - z_c \sim (\phi - \phi_c)^{1/2}$ [8]. At $T > 0$, the thermal motion breaks particle contacts frequently. Figure 3a shows that at p_j the coordination number z_j is even lower than z_c , although $\phi_j > \phi_c$, so the thermal motion breaks the jamming-like scaling of the coordination number. When the temperature drops, z_j gradually decreases. Meanwhile, the slope $(\frac{dz}{dp})_{z_j}$ grows rapidly to infinity in the $T = 0$ limit. This is consistent with the sudden jump of the coordination number from 0 to z_c at Point J [8].

Although the coordination number does not possess the jamming feature at $p > p_j$, its fluctuation δz^2 is peaked at p_j , as shown in Figure 3b. The drop of δz^2 at $p > p_j$ is another strong evidence of the formation of amorphous solids. At the low temperature limit, the peak value of δz^2 seems to saturate to a nonzero value, implying the singularity of Point J, because $\delta z^2 = 0$ at $T = 0$.

Isostaticity determines the special vibrational properties of marginally jammed solids [6, 9, 10, 14]. For in-

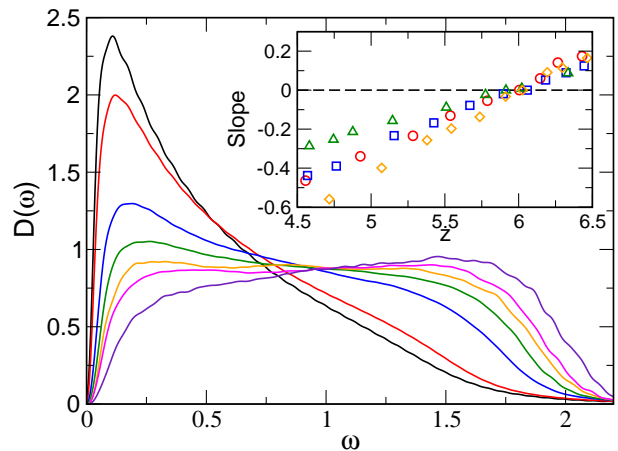


Figure 4 | Pressure dependence of the density of vibrational states at fixed temperature. The density of vibrational states, $D(\omega)$ in the main panel are for systems with harmonic ($\alpha = 2$) repulsion at $T = 10^{-5}$. The pressures are 0.0008, 0.001, 0.002, 0.003, 0.004, 0.005, and 0.009 from the black to violet curves. The inset shows the estimated slope of $D(\omega)$ in the intermediate frequency range versus the coordination number z for $T = 10^{-4}$ (red circles), 10^{-5} (blue squares), 10^{-6} (green triangles), and 10^{-7} (orange diamonds).

stance, the density of vibrational states, $D(\omega)$ possesses a low-frequency plateau at Point J, which shrinks with increasing $\phi - \phi_c$ and eventually disappears [6]. Is it likely that the isostaticity controls the flattening of $D(\omega)$ even at $T > 0$? As shown in Figure 4, the shape of $D(\omega)$ at $T > 0$ varies with the pressure. Interestingly, the plateau is formed in $D(\omega)$ at $p > p_j$. We estimate the average slope of $D(\omega)$ in the intermediate frequency regime and find that the flattening of $D(\omega)$ happens approximately at $z = z_c$, which confirms the strong coupling between the isostaticity and flattening of $D(\omega)$ even in thermal systems.

We show in Figure 5 a phase diagram to summarize our major findings. At fixed low temperature, the glass transition ($T_g \sim p/\phi^2$), jamming transition (emergence of g_1^{\max} , $T_j \sim (p/\phi^2)^{\alpha/(\alpha-1)}$), and isostaticity ($T_i \sim (p/\phi^2)^l$, where $l \approx 3.0$ for $\alpha = 2$ and 2.3 for $\alpha = 2.5$) occur in sequence with increasing the pressure. The jamming transition and isostaticity converges to Point J in the $T = 0$ limit, but not the glass transition. This separation implies the complexity of the formation of colloidal glasses. Recent studies have shown some puzzling non-monotonic dynamics below (beyond) the glass transition temperature (pressure) [26, 27], to some extent reflecting the ambiguity of the dynamically-defined glass transition and in agreement with the complexity shown in Figure 5. Compared to the uncertainty of the glass transition, the jamming transition has more definite structural and thermodynamic signs of the formation of amorphous solids. More importantly, the scaling laws observed at the jamming transition induce critical scaling collapse of multiple quantities, proposing the criticality of

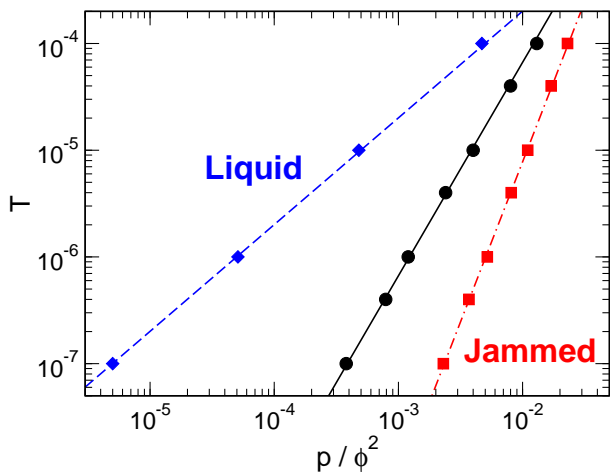


Figure 5 | Phase diagram of systems with harmonic ($\alpha = 2$) repulsion. The glass transition temperature (blue diamonds), jamming transition temperature (black circles), and isostaticity temperature (red squares) are plotted together as a function of the pressure divided by the square of the volume fraction, p/ϕ^2 . The lines are power-law fits to the data: $T_g \sim p/\phi^2$ (blue dashed), $T_j \sim (p/\phi^2)^2$ (black solid), and $T_i \sim (p/\phi^2)^3$ (red dot-dashed).

the $T = 0$ jamming transition at Point J. Moreover, the temperature and pressure dependence of the isostaticity calls for further studies, especially in experiments, to understand the meaning of the critical scaling exponent and the temperature and pressure evolution of the normal modes of vibration in amorphous solids, which may help to figure out the origin of the complicated dynamics.

Our conclusions are limited to low temperatures and pressures where the influence of Point J is still sensible. As shown in Figure 5, if the critical scalings hold at high temperatures, the three lines eventually get across. Recent studies have shown that the glass transition temperature drops with increasing the pressure at sufficiently high pressures [28], so nothing is predictable at high temperatures and pressures from the low-temperature and pressure properties. Beyond the

regimes concerned here, we will enter a new territory with completely new deep jamming pictures [29].

Methods

The systems studied here are three-dimensional cubic boxes consisting of $N = 1000$ spheres with the same mass m . Half of the spheres have a diameter σ , while the other half have a diameter 1.4σ , to avoid crystallization. Periodic boundary conditions are applied in all directions. Particles i and j interact via pairwise potential $V_{ij} = \frac{\epsilon}{\alpha} (1 - r_{ij}/\sigma_{ij})^\alpha$ when their separation r_{ij} is less than the sum of their radii σ_{ij} , and zero otherwise. Harmonic ($\alpha = 2$) and Hertzian ($\alpha = 5/2$) repulsions are studied. We set the units of mass, energy, and length to be m , ϵ , and σ , and the Boltzmann constant $k_B = 1$. The frequency is in the units of $\sqrt{\epsilon/m\sigma^2}$. We perform molecular dynamics simulations at constant temperature and pressure using Gear predictor-corrector algorithm. In the main context, we only show the results for harmonic repulsion. Supplementary Information contains the results for Hertzian repulsion.

The density of vibrational states is obtained from the Fourier transform of the velocity correlation $C(t) = \langle \vec{v}(t) \cdot \vec{v}(0) \rangle$ [30]:

$$D(\omega) = \frac{1}{3T} \int_0^\infty C(t) \cos(\omega t) dt,$$

where $\langle \cdot \rangle$ denotes the time and particle average.

The relaxation time τ is defined as the time at which the intermediate scattering function $F(t) = \frac{2}{N} \sum_j \exp(i\vec{k} \cdot (\vec{r}_j(t) - \vec{r}_j(0)))$ decays to e^{-1} , where the sum runs over all the large particles, and \vec{k} is chosen to be the value at the first peak of the static structure factor. The glass transition temperature, T_g is estimated from the Vogel-Fulcher fit of the relaxation time

$$\tau = \tau_0 \exp\left(\frac{A}{T - T_g}\right),$$

where τ_0 and A are fitting parameters.

[1] Zhang, Z., Xu, N., Chen, D. T. N., Yunker, P., Alsayed, A. M., Aptowicz, K. B., Habdas, P., Liu, A. J., Nagel, S. R. & Yodh, A. G. Thermal vestige of the zero-temperature jamming transition. *Nature* **459**, 230-233 (2009).

[2] Keys, A. S., Abate, A. R., Glotzer, S. C. & Durian, D. J. Measurement of growing dynamical length scales and prediction of the jamming transition in a granular material. *Nature Phys.* **3**, 260-264 (2007).

[3] Liu, A. & Nagel S. R. Nonlinear dynamics - Jamming is not just cool any more. *Nature* **396**, 21-22 (1998).

[4] Trappe, V., Prasad, V., Cipelletti, L., Segre, P. N. & Weitz, D. A. Jamming phase diagram for attractive particles. *Nature* **411**, 772-775 (2001).

[5] Song, C., Wang, P. & Makse, H. A. A phase diagram for jammed matter. *Nature* **453**, 629-632 (2008).

[6] Silbert, L. E., Liu, A. J. & Nagel, S. R. Vibrations and diverging length scales near the unjamming transition. *Phys. Rev. Lett.* **95**, 098301 (2005).

[7] Durian, D. J. Foam mechanics at the bubble scale. *Phys. Rev. Lett.* **75**, 4780-4783 (1995).

[8] O'Hern, C. S., Silbert, L. E., Liu, A. J. & Nagel, S. R. Jamming at zero temperature and zero applied stress: The epitome of disorder. *Phys. Rev. E* **68**, 011306 (2003).

[9] Wyart, M., Silbert, L. E., Nagel, S. R. & Witten T. A. Effects of compression on the vibrational modes of marginally jammed solids. *Phys. Rev. E* **72**, 051306 (2005).

- [10] Wyart, M., Nagel, S. R. & Witten, T. A. Geometric origin of excess low-frequency vibrational modes in weakly connected amorphous solids. *Europhys. Lett.* **72**, 486-492 (2005).
- [11] Ellenbroek, W. G., Somfai, E., van Hecke, M. & van Saarloos, W. Critical scaling in linear response of frictionless granular packings near jamming. *Phys. Rev. Lett.* **97**, 258001 (2006).
- [12] Olsson, P. & Teitel, S. Critical scaling of shear viscosity at the jamming transition. *Phys. Rev. Lett.* **99**, 178001 (2007).
- [13] Head, D. A. Critical scaling and aging in cooling systems near the jamming transition. *Phys. Rev. Lett.* **102**, 138001 (2009).
- [14] Xu, N., Vitelli, V., Wyart, M., Liu, A. J. & Nagel, S. R. Energy transport in jammed sphere packings. *Phys. Rev. Lett.* **102**, 038001 (2009).
- [15] Torquato, S. & Stillinger, F. H. Jammed hard-particle packings: From Kepler to Bernal and beyond. *Rev. Mod. Phys.* **82**, 2633-2672 (2010).
- [16] Chaudhuri, P., Berthier L. & Sastry S. Jamming transitions in amorphous packings of frictionless spheres occur over a continuous range of volume fractions. *Phys. Rev. Lett.* **104**, 165701 (2010).
- [17] Xu, N., Blawdziewicz, J. & O'Hern, C. S. Random close packing revisited: Ways to pack frictionless disks. *Phys. Rev. E* **71**, 061306 (2005).
- [18] Xu, N., Wyart, M., Liu, A. J. & Nagel, S. R. Excess vibrational modes and the boson peak in model glasses. *Phys. Rev. Lett.* **98**, 175502 (2007).
- [19] Debenedetti, P. G. & Stillinger, F. H. Supercooled liquids and the glass transition. *Nature* **410**, 259-267 (2001).
- [20] Berthier L. & Biroli G. Theoretical perspective on the glass transition and amorphous materials. *Rev. Mod. Phys.* **83**, 587-645 (2011).
- [21] Lerner, E., Procaccia, I. & Zylberg, J. Statistical mechanics and dynamics of a three-dimensional glass-forming system. *Phys. Rev. Lett.* **102**, 125701 (2009).
- [22] Tanaka, H., Kawasaki, T., Shintani, H. & Watanabe, K. Critical-like behavior of glass-forming liquids. *Nature Mater.* **9**, 324-331 (2010).
- [23] Silbert, L. E., Liu, A. J. & Nagel, S. R. Structural signature of the unjamming transition at zero temperature. *Phys. Rev. E* **73**, 041304 (2006).
- [24] Donev, A., Torquato, S. & Stillinger, F. H. Pair correlation function characteristics of nearly jammed disordered and ordered hard-sphere packings. *Phys. Rev. E* **71**, 011105 (2005).
- [25] Xu, N., Haxton, T. K., Liu, A. J. & Nagel, S. R. Equivalence of glass transition and colloidal glass transition in the hard-sphere limit. *Phys. Rev. Lett.* **103**, 245701 (2009).
- [26] Kob, W., Roldán-Vargas, S. & Berthier, L. Non-monotonic temperature evolution of dynamic correlations in glass-forming liquids. *Nature Phys.*, DOI: 10.1038/NPHYS2133 (2011).
- [27] Ballesta, P., Duri, A. & Cipelletti, L. Unexpected drop of dynamical heterogeneities in colloidal suspensions approaching the jamming transition. *Nature Phys.* **4**, 550-554 (2008).
- [28] Berthier, L., Moreno, A. J. & Szamel, G. Increasing the density melts ultrasoft colloidal glasses. *Phys. Rev. E* **82**, 060501(R) (2010).
- [29] Zhao, C., Tian, K. & Xu, N. New jamming scenario: From marginal jamming to deep jamming. *Phys. Rev. Lett.* **106**, 125503 (2011).
- [30] Keyes T. Instantaneous normal mode approach to liquid state dynamics. *J. Phys. Chem. A* **101**, 2921-2930 (1997).

Supplementary information

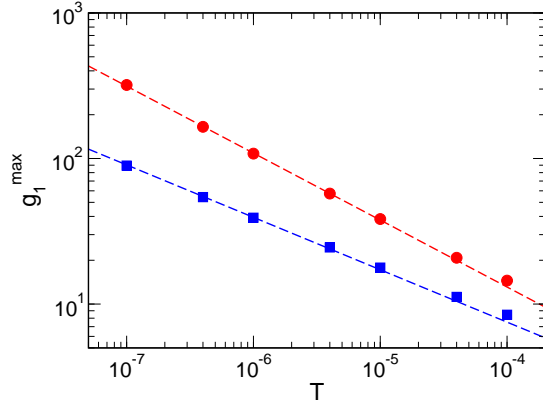


Figure 6 | Temperature dependence of the maximum value of the first peak of the pair distribution function, g_1^{\max} . The red circles and blue squares are for systems with harmonic ($\alpha = 2$) and Hertzian ($\alpha = 2.5$) repulsions, respectively. The red and blue dashed lines show the power law scalings: $g_1^{\max} \sim T^{-0.46}$ and $g_1^{\max} \sim T^{-0.36}$ ($g_1^{\max} \sim T^{-(0.90 \pm 0.02)/\alpha}$), respectively.

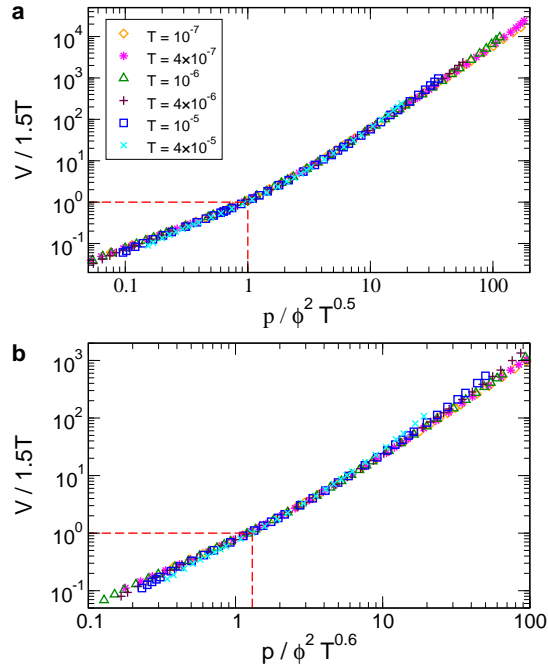


Figure 7 | Scaling collapse of the ratio of the potential energy per particle to the thermal energy, $V/\frac{3}{2}T$ for systems with **a**, harmonic ($\alpha = 2$) and **b**, Hertzian ($\alpha = 2.5$) repulsions. The pressure p is scaled by $\phi^2 T^{(\alpha-1)/\alpha}$. The red dashed lines mark the location at which $V = \frac{3}{2}T$, which is approximately at the emergence of g_1^{\max} .

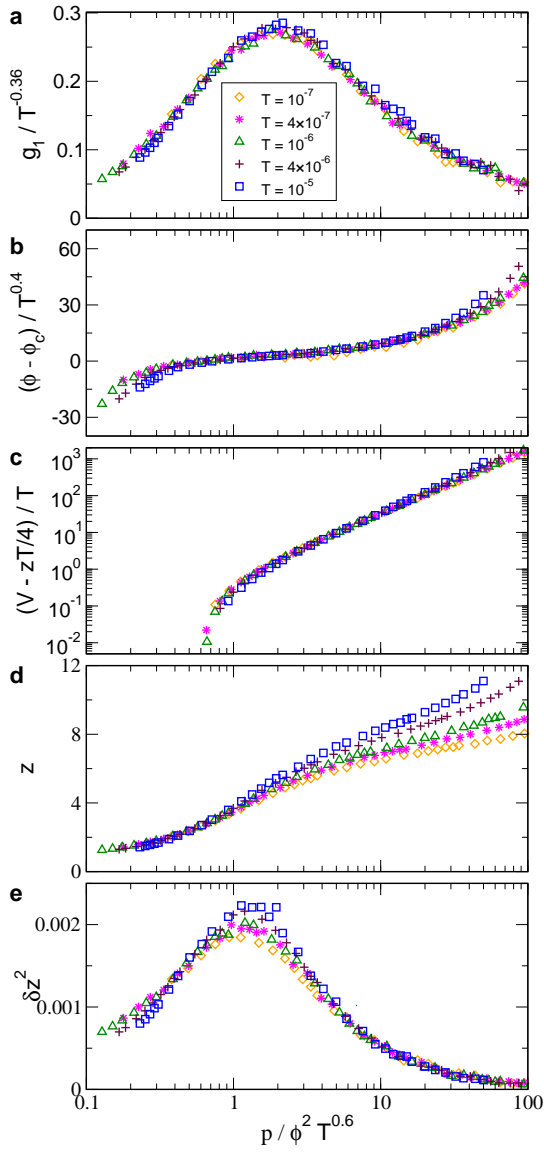


Figure 8 | **a**, The height of the first peak of the pair distribution function, g_1 scaled by $T^{-0.36}$, **b**, volume fraction difference from the $T = 0$ jamming transition, $\phi - \phi_c$ scaled by $T^{0.4}$, **c**, potential energy per particle subtracting the thermal contribution, $V - zT/4$ scaled by T , **d**, coordination number, z , and **e**, fluctuation of z , δz^2 versus the scaled pressure $p/\phi^2 T^{0.6}$ for systems with Hertzian ($\alpha = 2.5$) repulsion.

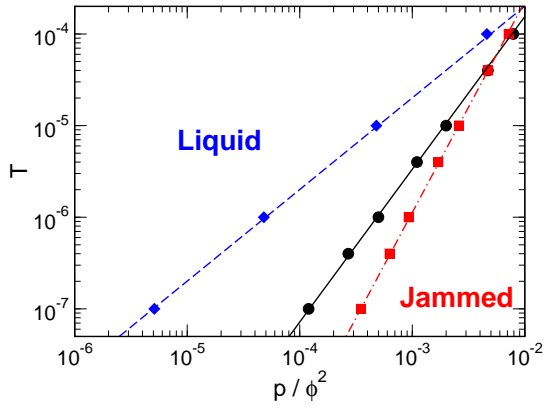


Figure 9 | Phase diagram of systems with Hertzian ($\alpha = 2.5$) repulsion. The glass transition temperature (blue diamonds), jamming transition temperature (black circles), and isostaticity temperature (red squares) are plotted together as a function of the pressure divided by the square of the volume fraction, p/ϕ^2 . The lines are power-law fits to the data: $T_g \sim p/\phi^2$ (blue dashed), $T_j \sim (p/\phi^2)^{5/3}$ (black solid), and $T_i \sim (p/\phi^2)^{2.3}$ (red dot-dashed).